clean technologies

MDPI

Article

Greenhouse Gas Implications of Extending the Service Life of PEM Fuel Cells for Automotive Applications: A Life Cycle Assessment

Alessandro Arrigoni [1], Valeria Arosio [2], Andrea Basso Peressut [2,*], Saverio Latorrata [2,*] and Giovanni Dotelli [2]

[1] Joint Research Centre (JRC), European Commission, 1755 LE Petten, The Netherlands; alessandro.arrigoni-marocco@ec.europa.eu
[2] Department of Chemistry, Materials and Chemical Engineering "Giulio Natta", Politecnico di Milano, Piazza Leonardo da Vinci 32, 20133 Milan, Italy; valeria.arosio@polimi.it (V.A.); giovanni.dotelli@polimi.it (G.D.)
* Correspondence: andreastefano.basso@polimi.it (A.B.P.); saverio.latorrata@polimi.it (S.L.)

Abstract: A larger adoption of hydrogen fuel-cell electric vehicles (FCEVs) is typically included in the strategies to decarbonize the transportation sector. This inclusion is supported by life-cycle assessments (LCAs), which show the potential greenhouse gas (GHG) emission benefit of replacing internal combustion engine vehicles with their fuel cell counterpart. However, the literature review performed in this study shows that the effects of durability and performance losses of fuel cells on the life-cycle environmental impact of the vehicle have rarely been assessed. Most of the LCAs assume a constant fuel consumption (ranging from 0.58 to 1.15 $kgH_2/100$ km) for the vehicles throughout their service life, which ranges in the assessments from 120,000 to 225,000 km. In this study, the effect of performance losses on the life-cycle GHG emissions of the vehicles was assessed based on laboratory experiments. Losses have the effect of increasing the life-cycle GHG emissions of the vehicle up to 13%. Moreover, this study attempted for the first time to investigate via laboratory analyses the GHG implications of replacing the hydrophobic polymer for the gas diffusion medium (GDM) of fuel cells to increase their durability. LCA showed that when the service life of the vehicle was fixed at 150,000 km, the GHG emission savings of using an FC with lower performance losses (i.e., FC coated with fluorinated ethylene propylene (FEP) instead of polytetrafluoroethylene (PTFE)) are negligible compared to the overall life-cycle impact of the vehicle. Both the GDM coating and the amount of hydrogen saved account for less than 2% of the GHG emissions arising during vehicle operation. On the other hand, when the service life of the vehicle depends on the operability of the fuel cell, the global warming potential per driven km of the FEP-based FCEV reduces by 7 to 32%. The range of results depends on several variables, such as the GHG emissions from hydrogen production and the initial fuel consumption of the vehicle. Higher GHG savings are expected from an FC vehicle with high consumption of hydrogen produced with fossil fuels. Based on the results, we recommend the inclusion of fuel-cell durability in future LCAs of FCEVs. We also advocate for more research on the real-life performance of fuel cells employing alternative materials.

Keywords: PEM fuel cell; durability; life-cycle assessment; PTFE; FEP; gas diffusion medium; GDL; MPL; global warming potential; greenhouse gas emissions

Citation: Arrigoni, A.; Arosio, V.; Basso Peressut, A.; Latorrata, S.; Dotelli, G. Greenhouse Gas Implications of Extending the Service Life of PEM Fuel Cells for Automotive Applications: A Life Cycle Assessment. *Clean Technol.* **2022**, *4*, 132–148. https://doi.org/10.3390/cleantechnol4010009

Academic Editors: Damien Guilbert and Gianpaolo Vitale

Received: 28 December 2021
Accepted: 11 February 2022
Published: 23 February 2022

1. Introduction

The deployment of fuel-cell electric vehicles (FCEVs) is typically included in public [1] and private [2] strategies to decarbonize the transportation sector. This inclusion is supported by life-cycle assessment (LCA) studies, which show the potential greenhouse gas (GHG) emission benefit of replacing internal combustion engine vehicles (ICEVs) with their fuel-cell counterpart. The promising environmental advantages of FCEVs compared to

ICEVs are the high efficiency of the fuel cells (FCs) and the almost null tailpipe pollutant emissions [3]. To be truly advantageous from an environmental perspective, however, FCEVs need to generate a lower impact throughout their life cycle [4]. In addition to the differences in the production phase, the impact of an FCEV is strictly dependent on the type and amount of fuel used during operation (i.e., fuel economy). Pure hydrogen-fed proton exchange-membrane FCs (PEMFCs) are the type of FCs typically employed for mobile applications thanks to their high output power density and low working temperature (60–80 °C) [5,6]. Hydrogen production and consumption are, therefore, key parameters in the LCA results of FCEVs [7]. While the life-cycle GHG emission implications of the hydrogen production pathway have been thoroughly investigated in the literature (e.g., [8,9]), less research has been put into the FC's role in influencing the effective amount of hydrogen consumed throughout the service life of the vehicle [10,11]. This deficiency leads to an oversimplification of the LCAs, and potentially to wrong conclusions. Our work aims to shed light on these crucial but still under-investigated parameters in the LCAs of FCEVs: fuel cell performance degradation with time, and durability. Moreover, based on laboratory results, the effect that these parameters have on the life-cycle GHG emissions of an FCEV is assessed.

The fuel economy of an FCEV throughout its service life depends on the driving cycle, the integration of the PEMFC with the energy storage systems on-board [12], and on the fuel cell performance. The latter depends on the initial performance of the FC, on its degradation rate, and eventually, on its replacement. A decreasing performance of PEMFCs over time can occur due to mechanical, chemical, or thermal degradation [13,14]. Indeed, durability is a critical issue for FCs compared to conventional energy generators [14]. According to commercial requirements, the lifetime of automotive FCs should be around 5000 h at the vehicle operating conditions [14]. However, while a lifetime of 30,000 h can be reached for stationary applications, a recent review stated that PEMFCs can only last 2500–3000 h in automotive applications [15].

The main components affected by durability issues are the electrolyte membrane, catalytic layers, and the gas diffusion medium (GDM). Failure and degradation of the electrolyte membrane can occur because of dimensional changes induced by relative humidity and temperature cycling, excessive flow rates of reactants, and chemical attack by undesired peroxides produced during the electrochemical process [14]. Moreover, inaccurate fabrication processes of the membrane electrode assembly (MEA) can generate cracks, tears, or holes that dramatically limit the durability of the whole device [14,16]. A Pt-based catalyst may lose its activity due to possible impurities (e.g., CO, S) in the reactants, which could irreversibly adsorb onto the electrode surface. Deactivation of the catalyst may also be induced by sintering or migration of Pt particles on the carbon support, detachment and dissolution into the electrolyte, and corrosion of the carbon support [16]. As for GDMs, the main degradation mechanisms are chemical and mechanical, whereas thermal degradation can be considered negligible [17].

The GDM is a fundamental component of a PEMFC: it consists of a carbon fiber-based macroporous substrate (gas diffusion layer, GDL) coated with a microporous layer (MPL) made of carbon nanoparticles and a hydrophobic agent, typically polytetrafluoroethylene (PTFE) [18]. It is located between the serpentines of the bipolar plate and the electrode, and it manages both water that enters the cell with humidified reactants and water that is generated by the electrochemical process. Hence, proper water management of FCs is crucial to their optimal functioning and to maintain constant efficiency [17]. However, unlike membranes and catalytic layers, standardized protocols to assess the durability of GDMs do not exist [14], which calls for the need to develop ad-hoc accelerated stress tests (ASTs) [13].

Chemical degradation of the GDM can be caused by polymer deterioration or carbon corrosion, inducing a slight reduction of hydrophobicity, while mechanical degradation is mainly due to the continuous gas flow in the presence of water, which can cause the detachment of the MPL carbon layer and its dissolution in water [13]. The latter is the most

crucial mechanism affecting the durability of GDMs. In fact, the loss of surface carbon of the MPL induced by both a gaseous stream and water production has been proven more detrimental than chemical degradation caused by the acidic environment [13]. The related performance losses can be limited with a further coating employing binder species able to enhance the adhesion between MPL and GDL, and to consequently avoid the detachment of the surface carbon particles [19]. A precaution concerning operating conditions could be the running of the fuel cell at medium-low relative humidities (not higher than 60%), thus reducing the water content in the device. Moreover, working points far from the concentration polarization region (i.e., high current-density values) should be preferred to limit the overproduction of water from the redox process, and to achieve a higher overall efficiency [13].

Considering the effect of the GDM degradation on the durability performance of an FC is, therefore, fundamental for a reliable evaluation of the environmental impact of the vehicle. This work investigates the role of GDM degradation via LCA for the first time. First, an extensive review of the scientific literature is performed to uncover how fuel-cell durability and performance losses are considered in the LCA studies of FCEVs. Then, supported by the experimental results acquired in previous work by the authors [13], the role of these parameters in affecting the LCA of an FCEV is investigated. For the aforementioned reasons, only the experimental results from mechanically stressed samples were used for the assessment. To assess how the mechanical degradation of GDM can be affected by the choice of the hydrophobic agent, the GHG implications of replacing PTFE with fluorinated ethylene propylene (FEP) are also investigated. In previous experiments, FEP proved to be capable of reducing mass-transfer resistances at a high current density, thus enhancing water management and output power [19,20]. Moreover, thanks to a lower melting point, the use of FEP allows us to decrease the sintering temperature of the coated GDM from 350 °C (for PTFE-based GDMs) down to 260 °C [21]. Despite these clear environmental benefits, the overall GHG consequences of replacing PTFE with FEP in the GDM of an FCEV have not been assessed before. The results of the present work are intended to provide new information for policymakers, scientists, and car manufacturers on the GHG emissions of FCEVs and suggest potential ways to reduce them.

2. Materials and Methods

2.1. Literature Review

A systematic review of how the durability of PEMFC is treated in LCA studies was performed. The research was limited to studies published after 2015 that performed a life-cycle assessment of passenger cars. In particular, the parameters reviewed were: the lifetime of the FCEVs, durability of the FCs, type of GDL used in the FCs, performance losses of the FCs with time, replacement of the FCs during the service life of the vehicles, and fuel economy of the vehicles. The results of the review are presented in Section 3.1.

2.2. GDMs' Preparation

To investigate how the GDM affects the durability of FCs, two cells with GDMs coated with different polymers were tested in the lab. Two fluorinated polymers, namely PTFE and FEP, were used as hydrophobic agents for both GDLs and MPLs. In previous works, FEP was shown to improve the water management of a common PEMFC at a high current density, allowing the device to achieve higher output power densities [19,20]. For the experimental study, commercial carbon fiber GDLs (SAATI Group) were immersed in a 1 wt.% polymeric suspension for 20 min and then subjected to a 30 min thermal treatment. During the latter, a temperature of 350 °C was reached for PTFE and 260 °C for FEP [20]. Once treated, 40 µm MPLs were deposited onto GDLs using the blade-coating technique with a linear velocity of 0.0154 m s^{-1}, corresponding to a shear rate of about 350 s^{-1}. The MPLs were prepared from inks containing both carbon black (Vulcan XC72R from Cabot, Cabot Italiana S.p.A., Ravenna, Italy) and multi-wall carbon nanotubes (CNTs, NTX1, Nanothinx, Patras, Greece) as the carbonaceous phase, the above-mentioned

hydrophobic fluorinated polymers, isopropyl alcohol as the dispersant, and water as the solvent. Inks were stirred at 8000 rpm for 10 min by the UltraTurrax T25 homogenizer (IKA GmbH, Staufen, Germany). After deposition, the resulting GDMs were treated for 30 min at the same temperature (350 °C and 260 °C for PTFE-based and for FEP-based samples, respectively) reached in the GDLs' hydrophobization stage to eliminate solvents and dispersants and consolidate the deposited carbon layers [20]. The other components of the tested fuel cell were fixed so that only the influence of the hydrophobic polymer agent on performance, durability, and sustainability was assessed. Specifically, graphitic bipolar plates (Ballard Fuel Cells), with a single serpentine in the anodic compartment and a triple one at the cathode, were adopted. A catalyst-coated membrane (Baltic Fuel Cells) was employed as the membrane electrode assembly with Nafion-212 electrolyte and Pt/C catalytic layers with a catalyst loading of 0.3 and 0.6 mg cm^{-2} at the anode and cathode, respectively.

2.3. PEMFCs' Performance Losses

The effect on durability of PTFE- and FEP-based GDMs was preliminarily evaluated in a previous work [13], where the fuel cell was kept at a constant current density (0.5 A cm^{-2}, which is a common working point for conventional devices [18]) for 1000 h at 60 °C and an 80–100% (anode-cathode) relative humidity. Polarization experiments were performed every 100 h feeding 0.25 NL min^{-1} of pure hydrogen and 1 NL min^{-1} of air to the anode and cathode, respectively. Such tests, however, are only slightly representative of the resistance against degradation during the service life of the device. Therefore, an ad-hoc accelerated stress test (AST) was performed to quicken the degradation of GDMs and avoid testing the fuel cell for thousands of hours. Among the possible degradation mechanisms that affect the performance of GDMs (i.e., chemical, mechanical, and thermal), the mechanical is the most detrimental, leading to the detachment of the surface carbon of the MPLs. For this reason, a mechanical AST was carried out by assembling the prepared GDMs in a dummy cell [13]. For the test, a Teflon film was used as a separator between the anode and cathode where the GDMs were assembled. To avoid distortion of the analysis and prevent potential electrochemical stress on the samples, hydrogen and catalysts were not used. Pressurized air was supplied continuously for 1000 h to each side of the cell, with a twofold flow rate compared to that employed for conventional tests (0.5 NL min^{-1} at the anode and 2 NL min^{-1} at the cathode).

After performing the AST, the stressed GDMs were assembled in a lab-scale fuel cell to obtain the polarization curves. The fuel cell was operated at 60 °C and 80–100% (anode-cathode) relative humidity with hydrogen (0.25 NL min^{-1}) and air (1 NL min^{-1}) supplied to the anode and cathode, respectively. The polarization curves were then compared to those obtained with fresh (i.e., not stressed) components to estimate the performance loss induced by the AST.

2.4. From Lab Results to Real-World Performance

In this section, we attempt to link the fuel consumption of single-cell laboratory tests to real-world operations. Considering the hydrogen flow rate that is needed to power an FC over a certain mileage, the corresponding current can be computed from Equation (1):

$$I = \frac{\dot{m}_{H_{2,cons}}}{MW_{H_2}} 2F \quad (1)$$

where $\dot{m}_{H_{2,cons}}$ [kg h^{-1}] is the stoichiometric mass flow rate of hydrogen (i.e., the amount of fuel consumed), MW_{H_2} [kg mol^{-1}] the molecular weight of hydrogen, and F [C mol^{-1}] the Faraday's constant. The current value I [A] is needed to find the corresponding working voltage for the lab-scale system assembled with PTFE- and FEP-treated samples. The voltage loss induced by the accelerated stress test is then considered: to keep a constant power output (V·I) while the cell is aging, the current must be increased. Higher currents

lead to higher hydrogen consumption levels. Figure 1 shows the degradation performances of the two cells tested in the lab: since FEP-based GDMs can limit the degradation rate ($\mu V\ h^{-1}$) compared to PTFE, they are also supposed to reduce the hydrogen consumption.

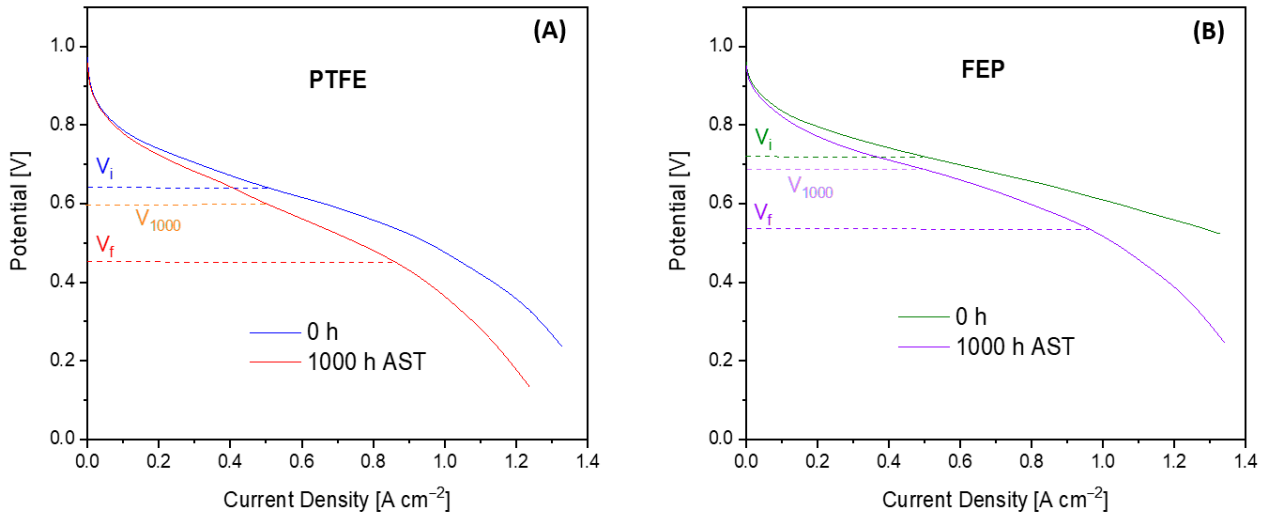

Figure 1. Polarization curves of the single cell assembled with fresh (0 h) and stressed (1000 h AST) PTFE- (**A**) or FEP-based (**B**) GDMs. AST: accelerated stress test.

The experimental data were used to get the real-world degradation rates for the GDMs and estimate the total lifetime of the FC. Table 1 reports the voltage values obtained from the polarization curves reported in Figure 1 (i.e., the voltage at 0.5 A cm^{-2} from a single-lab-scale FC assembled with both fresh (V_i) and aged (V_{1000}) materials), the current density needed to keep the power constant, the corresponding hydrogen flow rates, and the lifetime. The lifetime (t_l [h]) was calculated with Equation (2) as the ratio between the voltage difference and the degradation rate DR [$\mu V\ h^{-1}$]. The values corresponding to the limit of the ohmic zone (0.45 V for PTFE and 0.52 V for FEP) were considered as final voltages (V_f in Figure 1). The method adopted here draws on the work by Chen et al. [22], who defined three load areas (low, transient, and high) for different operating conditions. Start-stop and idling conditions are allocated to the transient area, while the high load region is related to high-power operations, such as acceleration and high speed. Operating the FC beyond the high load area is considered too demanding for both materials and distribution equipment [22].

$$t_l = \frac{V_i - V_f}{DR}\ [\text{h}] \tag{2}$$

Table 1. Accelerated stress test (AST) experimental results for PTFE- and FEP-based single-lab-scale fuel cells. *DR*: degradation rate.

GDM	V_i	V_{1000}	DR	P	i	H_2	Lifetime
	[V]	[V]	[$\mu V\ h^{-1}$]	[W cm^{-2}]	[A cm^{-2}]	[NL min^{-1}]	[h]
PTFE	0.639	0.593	46	0.320	0.71	0.124	4109
FEP	0.718	0.687	31	0.359	0.69	0.120	6387

Based on the described approach, the reduction in hydrogen consumption (in terms of flow rate) is estimated to be around 3% when running a real lab-scale fuel cell assembled with FEP instead of PTFE after the accelerated stress test. Two cases were considered to link the single-cell data to the real-world performance of an FC stack composed of several cells: best-case (low-consumption) and worst-case (high-consumption). They are defined by the combination of the power density output and initial fuel consumption. Four references

were used to define the extreme scenarios: the minimum and maximum power densities (0.64 and 0.91 W cm^{-2}) came from Evangelisti et al. [23] and Benitez et al. [24], and the minimum and maximum initial fuel consumptions (0.58 and 1.15 $kgH_2/100$ km) from Huss et al. [25] and Frank et al. [26], respectively. Both PTFE- and PEF-based vehicles are assumed to start from the same initial fuel consumption, and they increase it with time in response to the performance losses measured in the lab. Assuming a constant performance degradation, the baseline FC (PTFE-based) reaches the critical ohmic zone limit after 4109 h (Table 1). This performance is within the same order of magnitude of the 5000 h for a 2020 FCEV reported by Hill et al. [9]. On the other hand, the FEP-based FC reaches the critical ohmic zone limit after 6387 h, lasting approximately 50% longer than its PTFE-based counterpart. If the baseline vehicle has a typical service life of 150,000 km, corresponding to an average velocity of about 36.5 km h^{-1} (e.g., [23,27]), the FEP-based FC reaches its end of life after 233,180 km. Therefore, the initial hydrogen consumption of the single cell is calculated from the ratio between the molar flow rate needed to power the FC at the initial current density (computed from the reference power density) and the average velocity. From the initial hydrogen consumption, the number of cells needed (N_c) can be calculated as reported in Equation (3), considering that the minimum and maximum initial consumptions of the reference stack correspond to 0.58 [25] and 1.15 [26] $kgH_2/100$ km, respectively:

$$N_c = \frac{Consumption\ reference\ stack}{Initial\ consumption_{H_2,t=0,single\ cell}} \quad (3)$$

The end-of-life consumption (i.e., at 150,000 km for the PTFE-based vehicle and 233,180 for the FEP-based one) was calculated considering the increase in the hydrogen molar flow rate needed to keep the power constant (Equations (4) and (5)):

$$m_{H_2,fin,stack} = \dot{n}_{H_2,fin} \cdot S \cdot MW_{H_2} \cdot t_l \cdot N_c \ [\mathrm{kg}] \quad (4)$$

$$Final\ consumption_{H_2,fin,s.c.} = \frac{m_{H_2,fin,stack}}{km_{tot}} 100 \left[\frac{\mathrm{kg_{H_2}}}{100\mathrm{km}}\right] \quad (5)$$

where $\dot{n}_{H_2,fin}$ [mol cm^{-2} h^{-1}] is the specific stoichiometric molar flow rate of hydrogen at the end of the service life of the FC, S [cm^2] is the electrode active area, t_l [h] is the lifetime of the FC estimated from the accelerated stress test (Table 1), and $m_{H_2,fin,stack}$ [kg] is the cumulative hydrogen consumption.

Table 2 summarizes the results for the low- and high-consumption cases in terms of the number of cells, the total area of GDMs needed, and fuel consumption. An electrode active area of 100 cm^2 was assumed to calculate the total area of the GDMs.

Table 2. Fuel-cell parameters and fuel consumption (initial, final, and cumulative) for the two fuel cells (PTFE- and FEP-based) in the low- and high-consumption cases. The values for FEP refer to the consumption after 4109 h (150,000 km), and in parenthesis, to the consumption after 6387 h (233,180 km).

Case	Power Density	N_{cell}	$A_{tot,GDL}$	Fuel Consumption				
				Initial	Final PTFE	Final FEP	Cumulative PTFE	Cumulative FEP
	[W cm^{-2}]		[m^2]	[$kgH_2/100$ km]			[kgH_2, tot]	
Low consumption	0.64 [a]/0.91 [b]	57/40	1.14/0.8	0.58 [c]	0.824	0.801 (0.924)	1053	1036 (1753)
High consumption	0.64 [a]/0.91 [b]	112/79	2.24/1.58	1.15 [d]	1.63	1.59 (1.83)	2087	2053 (3476)

a. [23], b. [24], c. [25], d. [26].

2.5. Global Warming Potential

This section of the article focuses on the methodology adopted for the LCA, in accordance with ISO standards 14040 [28] and 14044 [29].

2.5.1. Goal and Scope

The goals of this LCA are twofold: (1) to assess the GHG implications of including the performance losses of FCs in the LCA of an FCEV; (2) to assess the GHG implications of replacing PTFE with FEP in the GDMs of FCs for FCEVs. Two vehicles are compared across the entire life cycle (i.e., from cradle to grave): one where the GDM is coated with PTFE (i.e., reference vehicle), and one where the GDM is coated with FEP. A different GDM affects the emissions of a vehicle throughout its life cycle: from the production phase (emissions affected using different materials), through the use phase (emissions affected by the different hydrogen consumption levels when operating the vehicle), to the end-of-life phase (emissions delayed by the differential durability of the FCs). The system boundary of the study is illustrated in Figure 2. The functional unit of this study is one kilometer traveled by the vehicle (i.e., one vehicle-kilometer (vkm)). The LCA is performed with the software SimaPro 9.1, and ecoinvent 3.6 (cut-off system model) is used as the background database. Climate change is the only environmental impact category analyzed in the study, and the impact is quantified over a time horizon of 100 years. The characterization factors for the 100-year global warming potential (GWP100) are from the 5th assessment report of the Intergovernmental Panel on Climate Change [30]. All GHG emissions arising from the life cycle of the vehicle are assumed to occur at year zero. Therefore, the GHG emissions occurring at a delayed time (e.g., end-of-life emissions delayed thanks to the extension of the service life of the vehicle) are not discounted based on the shorter time they will warm the planet in the time horizon considered.

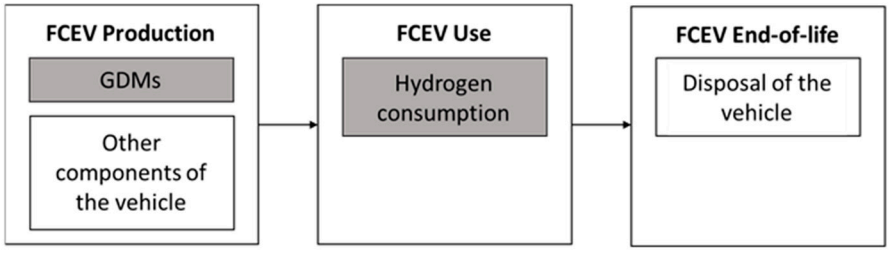

Figure 2. System boundaries of the LCA. Grey boxes indicate the phases of the vehicle life cycle that were considered in scenario A, while in scenario B all the phases (i.e., both grey and white boxes) were included in the assessment.

Two scenarios may be considered, and to explore those, different sensitivity analyses were performed on crucial fuel-cell parameters. The scenarios differ in the end-of-life stage: in scenario A, both vehicles are assumed to be disposed of after 150,000 km in accordance with the typical lifespan of vehicles reported in the literature [23,24,31,32]. In scenario B, the reference vehicle is assumed to be disposed of after 150,000 km, while for the FEP-based vehicle this occurs after 233,180 km. The latter value may be calculated from our experimental results, considering the lifetime of the FEP-coated GDM results to be 1.55 times longer than the GDM coated with PTFE (i.e., 6387 h vs. 4109 h, as reported in Table 1). Scenario A aims to investigate how the performance losses of the FC affect the LCA of the vehicle, and how the different GDMs affect the production phase and the hydrogen consumption of the vehicle during the operational phase. On the other hand, scenario B aims to assess the potential implication of extending the service life of the vehicle by improving the durability of the FC using FEP. Regarding vehicle production, the manufacture of all the vehicle components but the FC is assumed to be independent of the polymer used in the GDMs. In our work, sensitivity analyses on fuel-cell parameters, the initial fuel consumption, and hydrogen production technologies were performed with the aim of analyzing the variability of results due to the variation of input parameters. Regarding cell parameters, two different power densities (i.e., 0.64 W cm^{-2} and 0.91 W cm^{-2}) were investigated; these values were selected to assess the best and worst cases, as explained in Section 2.4. The same approach was adopted for the initial fuel consumption (0.58 and 1.15 kgH_2/100 km), using the lowest

and highest values found in the literature (see Table 3). The four combinations of power densities and initial fuel consumptions examined correspond to four different numbers of cells, and therefore, four different areas of the GDMs (see Table 2 for the values considered). Three hydrogen production pathways are considered for the operation phase of the vehicles: (i) electrolysis powered by the average European electricity mix; (ii) electrolysis powered by renewable electricity; (iii) steam methane reforming. The potential impacts are assessed for all the possible combinations of power densities, initial fuel consumption, and hydrogen production pathways.

2.5.2. Life-Cycle Inventory: Vehicle Product System

The only difference in the production stage of the compared vehicles is the fabrication of the GDM.

Gas Diffusion Medium

The production of the GDM can be divided into three main steps: (i) synthesis of the following monomers: tetrafluoroethylene (TFE) used for PTFE production, and TFE and hexafluoropropylene (HFP) for FEP production; (ii) polymerization; (iii) preparation of the GDM: i.e., coating of the carbon cloth with the selected polymer, and thermal treatment. In our work, the synthesis of the TFE monomer available on ecoinvent 3.6 was used for the assessment, while the inventory for HFP production was based on the information reported by Rodriguez et al. [33]. In their report, HFP is produced via combined pyrolysis of TFE and HFC-23. Input and output flows of the HFP manufacturing process are specified in the Supplementary Material (see Table S2). Mass-based allocation was performed to divide the energy inputs between the two co-produced monomers (TFE and HFP). The number of co-products was based on the annual production of the factory and on additional references [33,34]. Where precise information about the FEP manufacturing process was not available (i.e., emitted GHGs), conservative assumptions were made (see Section S2.1). The efficiency of the PTFE and FEP polymerization processes (see Tables S1 and S2) was based on Rodriguez et al. [33]. The consumption of water, initiators, and surfactants was neglected since they were assumed to be the same for the two polymers. As for the coating process, the immersion of the carbon fibers into a polymeric suspension and the subsequent thermal treatment were modeled. The amount of polymer on the carbon cloth material (34 wt.%) was calculated by weighting the GDL before and after the coating treatment. The electrical energy necessary for the thermal treatment was calculated from the different temperatures required in the lab to treat the two polymers: i.e., 350 °C for PTFE and 260 °C for FEP (see the Supplementary Information for the calculations performed to obtain the energy consumption).

Vehicle Manufacture and End of Life

The GWP impact of these phases was based on results found in the literature. The average impacts reported in four studies [23,24,31,35] were considered, and sensitivity analysis using the different values reported in the four studies was also performed. According to the literature, the overall impact of manufacturing and disposing of a passenger car ranges from 1.20 t CO_2 eq. [31] to 15.5 t CO_2 eq. [24], with an average value of 14.5 t CO_2 eq. Since the GHG emissions from vehicle manufacturing were sourced from the literature, the same impact was considered for the two compared vehicles (i.e., only the GDM impact on the operational phase of the vehicle was assessed).

2.5.3. Life-Cycle Inventory: Use Phase

In the use phase, only the impacts of hydrogen consumption are considered. The amount of hydrogen consumed was experimentally calculated as explained in Section 2.4. The fuel consumptions shown in Table 2 were used for the assessment. Hydrogen production via different pathways was modeled based on Bieker et al. [36]. In their study, the electricity consumption for hydrogen production via electrolysis (including compression

and dispensing) amounted to 1.68 MJ per MJ of hydrogen [36]. The life-cycle carbon intensity of EU electricity was set by Bieker et al. as 199 g of CO_2 eq. kWh^{-1} [36], assuming that the electricity mix during the service life of the vehicle will progressively decarbonize. The vehicle was assumed to start operating in 2021, and the Stated Policy Scenario of the IEA's World Energy Outlook was used for the estimate [37]. The carbon intensity of the EU renewable energy was estimated to be 23 g of CO_2 eq. kWh^{-1}, considering a mix composed of 33% of solar energy and 67% of wind energy [36]. Finally, the carbon intensity of hydrogen production via steam reforming was assumed to be 113 g of CO_2 eq. MJ^{-1} of hydrogen [36]. A lower heating value for hydrogen of 120 MJ kgH_2^{-1} and an electrolyzer efficiency of 57 kWh kgH_2^{-1} were assumed for the study [36]. Maintenance and tire emissions were neglected since previous studies showed their role in the life-cycle impacts to be trivial [9].

3. Results and Discussion

3.1. Literature Review

Results of the literature review are summarized in Table 3, where the primary assumptions made in the different studies are reported. If the reviewed studies made a sensitivity analysis of the parameters here investigated, for readability purposes, the variation of the values is presented in this section but not in the table. Since 2015, 19 studies were found in the literature that assessed the life-cycle environmental performances of FCEVs. All studies reported the fuel economy of the FCEV, with a range from 0.58 [25] to 1.15 kgH_2/100 km [26]. These extreme values were the ones used in the present analysis to calculate the impacts for the low- and high-consumption cases. The minimum consumption value was obtained from version 5 of the European Commission JEC Well-to-Wheels analysis. Low consumption was ascribed to the lower driving resistance of the vehicle segment compared to the FCEVs available on the market [25]. The other end of the fuel economy spectrum was calculated from the fuel efficiency of FC light-duty vehicles available in the GREET model (1.38 MJ km^{-1}) [26,38]. Most assessments used secondary data for the average fuel consumption of the vehicles. Often, the initial fuel economy provided by the car manufacturer was used for the analysis; therefore, the fuel consumption considered was lower than that experienced in real-life conditions. For instance, the FCEVs monitored in the framework of the European project H2ME had an average fuel consumption of 1.11 kgH_2/100 km in Germany and 1.26 kgH_2/100 km in Denmark [39]. These values are considerably higher than the average consumption assumed in the reviewed studies: 0.92 kgH_2/100 km. Real-life consumption results are also higher than those calculated from standardized driving cycles: for instance, Hwang et al. obtained a consumption of 0.96 kgH_2/100 km when considering the New European Driving Cycle (EUDC) [7]. Overall, the fuel economy seems to depend more on the driving conditions than the FC system [32]. In their study, Simons and Bauer forecasted an overall improvement in the fuel efficiency of only 0.2% in 10 years [32].

Although every study reported the amount of hydrogen consumed per 100 km, less information was provided regarding the durability of the FC and its effect on the fuel economy of the vehicle. The most covered parameter related to durability was the lifetime of the vehicle, which ranged from a maximum of 190,000 km [40,41], retrieved from the 2017 budget of the Fuel Cell Technology Office of the US Department of Energy [42], to a minimum of 120,000 km. The latter value was provided by Ahmadi et al. [10], who accounted for the performance losses of the FC due to repeated stops and starts. A degradation rate of 2.65×10^{-5} Vh^{-1} (Chen et al. [22]) from an initial cell voltage of 0.78 V was considered, and the FC was assumed to be usable for 12,000 h or until the voltage dropped below 0.5 V (i.e., 10,600 h of operation with the aforementioned degradation rate). In the other studies reviewed, the service life of the FC either was not mentioned or was assumed to be the same as the vehicle. The exceptions were the studies from Hill et al. [9] and Kannangara et al. [43]. Hill et al. assumed the service life of the FC in 2020 to be 5000 h, corresponding to a lifetime of the vehicle of more than 225,000 km [9]. The value for the

durability of the FC was validated by stakeholder experts, and future projections were also developed to account for changes in technology [9]. According to the projections, the service life of FCs is expected to reach 10,000 h in 2050. This value for 2050 is lower than the one Ahmadi et al. assumed for 2020. Kannangara et al. assumed the service life of the FC to be 150,000 km, and a lifetime vehicle mileage of 150,000–200,000 km. In the case where the operating mileage is above 150,000 km, the FC stack components are assumed to be replaced [43]. Sensitivity analyses including the replacement of the fuel cell and/or different mileages for the vehicle were carried out in other studies, too (e.g., [9,31,44]). Several studies included the environmental impacts of the maintenance of the vehicle, but none provided information regarding the maintenance of the FC. The main reason for this deficiency is the uncertainty related to real-world FC performance [24]. Nevertheless, the capacity of the FC is not expected to deteriorate by more than 15% in 10 years [32].

As mentioned earlier, Ahmadi et al. provided the only study to assess the GHG impact of the performance loss of the FCEV [10]. From an initial consumption of 1.1 kgH_2/100 km, based on the 2018 Toyota Mirai performance specifications, they found a reduction of the fuel economy (averaged over the 120,000 km lifetime of the vehicle) of 10–15 km per kg of hydrogen, depending on the driving pattern. As a consequence, the lifetime GHG emissions of the vehicle increased on average by 3200 kg CO_2 eq.

As for the fuel-cell components, most LCA studies used secondary data for the inventory of the GDM. The most referenced papers are the ones from Simons and Bauer [32], Miotti et al. [31], and Evangelisti et al. [23]. Simons and Bauer [32] modeled a GDM composed of a macroporous layer of woven carbon cloth hydrophobically treated with PTFE (15% loading), and a microporous layer of carbon (or graphite) particles mixed with PTFE binder. Similarly, Miotti et al. [31] considered a GDL composed of a 0.28-mm non-woven carbon substrate macroporous layer with a 0.04-mm microporous layer of PTFE and carbon black. The thicknesses are expected to reduce in the future, but the authors also consider the use of PTFE in 2030 and 2050. Finally, Evangelisti et al. [23] considered, for the baseline scenario, a GDM composed of a carbon cloth material coated with 10 wt.% PTFE and 5 wt.% of carbon black for the microporous layer. A complete LCA of the fuel cell system was also provided by Usai et al. [45]. In their case, the GDM results were lighter and thinner (0.21 mm with a density of 0.45 g cm^{-3}) than those in the aforementioned studies. Yet, the GDL (produced from polyacrylonitrile) was again assumed to be treated with PTFE (15 wt.%) to enhance its water management.

3.2. LCA

In this section, first, the results for scenario A (i.e., both vehicles disposed of after 150,000 km) are presented, followed by the results for scenario B (i.e., a vehicle with PTFE-based GDMs disposed of after 150,000 km and a vehicle with FEP-based GDMs disposed of after 233,180 km).

3.2.1. Scenario A

Performance losses of the fuel cell affect the hydrogen consumption of the vehicle throughout its service life, and therefore, its carbon footprint. Compared to a case where hydrogen consumption remained constant until the end-of-life (i.e., the typical assumption adopted in the LCAs of FCEVs found in the literature), the reference vehicle consumed from 183 to 362 kg of additional hydrogen. This consumption corresponds to an additional emission of 0.2–4.9 t CO_2 eq. If compared to the life cycle of the vehicle, including production and end-of-life, this equals an increase of 1–13%. The variation in the increased emissions depends on the initial fuel consumption and the pathway for hydrogen production. The change in the GHG performance is less marked in the case of hydrogen produced via electrolysis powered by renewable energy (i.e., less than 3 g CO_2 eq. per km). This is due to the lower GHG impact of hydrogen production, which reduces the impact of using more hydrogen. In the case of electrolysis powered by the EU electricity mix, the additional emissions amount to 14–27 g of CO_2 eq. km^{-1} (up to 4 t CO_2 eq. for the whole

service life), depending on the initial fuel consumption considered. The highest impact variation is noticed when hydrogen is produced via steam methane reforming. In this case, performance losses lead to an increase in the emissions of up to 4.9 t CO_2 eq. over the entire service life of the vehicle. The higher savings in this case are due to the high carbon intensity of hydrogen produced from fossil fuels.

Table 3. Literature review results. * Plug-in hybrid fuel cell battery vehicle. ** The value has been recently updated to 0.91 [46].

Reference	Year	EV Lifetime [km]	FC Lifetime	GDL	FC Losses	Replacement	Fuel Economy [kgH_2/100 km]
Ahmadi and Kjeang [11]	2015	180,000	N/A	N/A	N/A	N/A	0.78
Ahmadi et al. [10]	2020	120,000	12,000 h	N/A	2.65×10^{-5} Vh^{-1}	No	1.10
Bekel and Pauliuk [35]	2019	150,000	N/A	N/A	N/A	No	0.94
Benitez et al. [24]	2021	150,000	N/A	PTFE	N/A	No	0.76
Burkhardt et al. [47]	2016	N/A	N/A	N/A	N/A	N/A	0.97
Candelaresi et al. [40]	2021	190,000	190,000 km	N/A	N/A	No	0.76
Evangelisti et al. [23]	2017	150,000	N/A	PTFE	N/A	No	0.85
Frank et al. [26]	2021	N/A	N/A	N/A	N/A	N/A	1.15
Hill et al. [9]	2020	225,000	5000 h	N/A	N/A	No	1.06 **
Huss et al. [25]	2020	N/A	N/A	N/A	N/A	N/A	0.58
Kannangara et al. [43]	2021	150,000	150,000 km	N/A	N/A	No	0.94
Lombardi et al. [48] *	2017	200,000	N/A	N/A	N/A	N/A	0.72
Notter et al. [27]	2015	150,000	N/A	PTFE	N/A	No	0.85
Ren et al. [49]	2020	N/A	N/A	N/A	N/A	N/A	0.94
Sinha and Brophy [50]	2021	150,000	N/A	N/A	N/A	No	1.00
Simons and Bauer [32]	2015	150,000	150,000 km	PTFE	N/A	No	1.03
Usai et al. [45]	2021	N/A	N/A	PTFE	N/A	N/A	1.00
Velandia, Vargas, and Seabra [51]	2021	150,000	N/A	N/A	N/A	No	1.05
Yang et al. [44]	2020	150,000	N/A	N/A	N/A	N/A	1.05

Focusing on GDM manufacturing, the production of FEP-based GDMs results in a GWP higher than PTFE-based GDMs. This is mainly because PTFE is a TFE homopolymer, while FEP also contains HFP. The latter is produced via pyrolysis of HFC-23 and TFE, and therefore, requires an additional process with additional energy consumption. Nevertheless, the GWP impact variation in the manufacture of FEP and PTFE is almost negligible if compared to the impacts of the use phase of the vehicle. When the total GDL area of the FC is considered, the impact variation is in the order of 0.001 g CO_2 eq. km^{-1}. On the other hand, substituting PTFE- with FEP-based GDMs allows a saving of from 0.1 to 3.1 g CO_2 eq. per km during the use phase of the vehicle, corresponding to a GWP reduction of from 22 to 459 kg CO_2 eq. over the whole lifetime mileage (i.e., 150,000 km). As for the previous comparison with a hypothetical vehicle without performance losses, the higher GHG savings when using FEP (i.e., 3.1 g CO_2 eq. km^{-1}, corresponding to an overall saving of 459 kg CO_2 eq.) are obtained when hydrogen is produced via steam methane reforming. Conversely, the lowest savings from the use of FEP compared to the PTFE-based reference vehicle are obtained when hydrogen is assumed to be produced via renewable electrolysis (i.e., less than 0.3 g CO_2 eq. per km). In summary, substituting PTFE- with FEP-based GDMs allows the GHG emissions to be reduced by 10% due to performance losses.

Figure 3 shows the GWP reduction when using PEF-coated GDMs over the whole vehicle life cycle. The difference over the entire life cycle almost coincides with that of the use phase due to the negligibility of the impact of GDM production. The GWP reduction corresponds to a relative decrease of approximately 1.6% of the use-phase impacts.

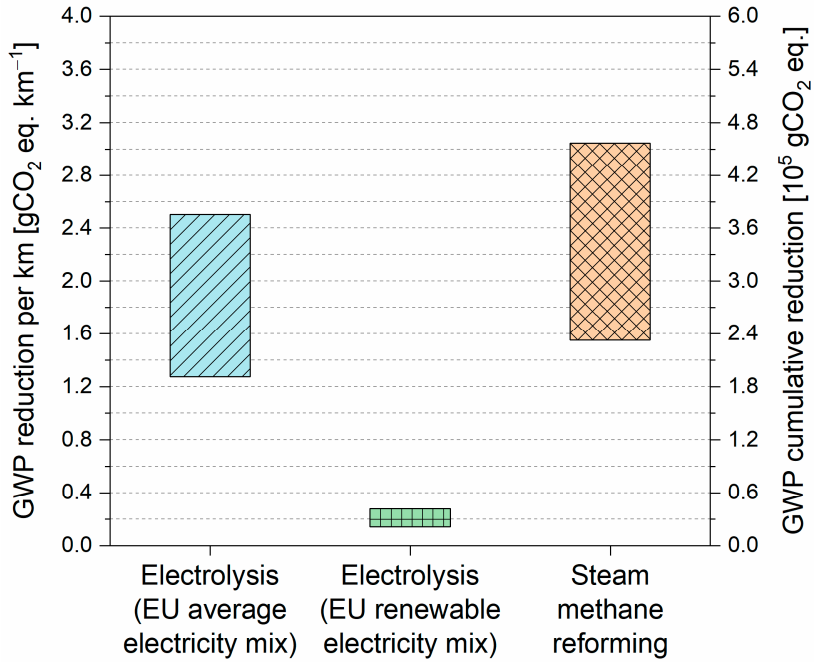

Figure 3. Global warming potential reduction per km (left *y*-axis) and over the entire life cycle (right *y*-axis) when substituting PTFE- with FEP-based GDMs in an FCEV. The reduction is calculated as the difference between the GWP for the PTFE-based FCEV and the GWP for the FEP-based FCEV. Floating bars represent the range of values obtained for each production pathway by varying the initial fuel consumption and the cell power densities.

3.2.2. Scenario B

In this scenario, an increase in the lifetime mileage of the vehicle with FEP-based GDMs is considered based on the assumption that a slower degradation of the FC leads to a longer service life of the entire vehicle. For this reason, the impact of the vehicle system (i.e., manufacturing and end of life) is distributed over a longer lifetime (i.e., 233,180 km) for the FEP vehicle with respect to the reference vehicle (i.e., 150,000 km). The resulting normalized impact of the vehicle system is 96.7 g CO_2 eq. km^{-1} for the PTFE-based vehicle and 62.2 g CO_2 eq. km^{-1} for the FEP-based vehicle.

The impacts of the use phase per driven km are higher in the case of FEP than for PTFE. Considering an initial fuel economy of 0.58 kgH_2/100 km, the impact is higher by 0.6–6.8 g CO_2 eq. km^{-1} depending on the hydrogen production pathway. When an initial fuel consumption of 1.15 kgH_2/100 km is considered, the difference between the impacts of FEP and PTFE increases: from 1.3 kg CO_2 eq. km^{-1} in the case of hydrogen produced via electrolysis with renewable electricity, to 13.4 kg CO_2 eq. km^{-1} in the case of hydrogen from steam methane reforming. The FEP-based vehicle has a higher GWP impact per km during the use phase due to the high fuel consumption in the last kilometers of its service life (approximately 80,000 km longer than the reference vehicle). As a result, the average fuel consumption during the entire life of the vehicle is higher.

Despite the higher impact of the use phase, the overall life-cycle GWP impact of the FEP vehicle is lower than that for the PTFE vehicle for all the analyzed fuel production pathways and cell parameters. The benefit of extending the lifetime mileage of the vehicle, in fact, overcomes the drawbacks of the higher fuel consumption in the last kilometers of the service life. Specifically, the introduction of FEP allows the impact to be reduced for an amount ranging from 15 to 36 g of CO_2 eq. per km, depending on FC features and hydrogen production pathways. The greatest benefit can be noted in the case of hydrogen produced via electrolysis powered by renewable sources (i.e., a GWP impact decrease by 27–37 g CO_2 eq. km^{-1}), as the GHG emissions near the end of life of the FEP vehicle are lower in this case. When hydrogen is sourced from electrolysis powered by the

EU electricity mix, the GWP difference between an FEP- and PTFE-based vehicle ranges from 17 to 33 g of CO_2 eq. per km. Finally, in the case of hydrogen from steam methane reforming, the GWP difference between the vehicles ranges from 15 to 31 g CO_2 eq. per km. Figure 4 shows the percentage of GWP reduction that would occur if PTFE-based GDMs were substituted with FEP-based ones. The GHG impact decreases from a minimum of 7.4% (in the case of hydrogen produced via steam methane reforming) to a maximum of 32% (in the case of hydrogen from electrolysis powered by renewable electricity mix).

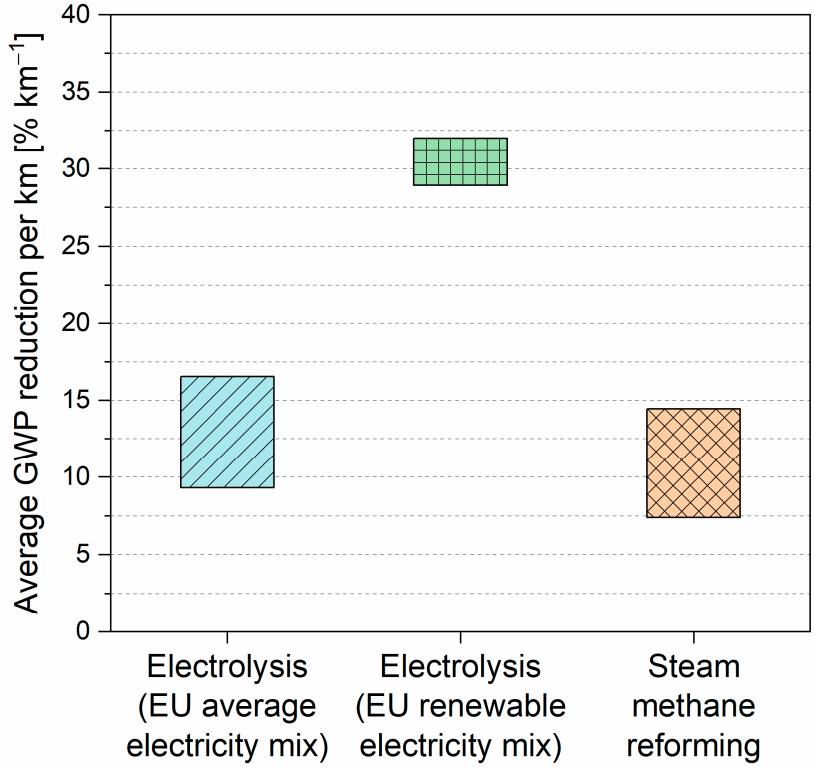

Figure 4. Global warming potential reduction (%) resulting from the substitution of PTFE-based GDMs with FEP-based ones. The GWP reduction is calculated as the percentage decrease with respect to the GWP of PTFE-based GDMs (assumed as a reference case). Floating bars illustrate the range of reduction for each hydrogen production pathway, obtained by varying the initial fuel consumption and considering different impacts for vehicle production and disposal phases.

4. Conclusions

The goal of this study was to investigate the role of fuel-cell performance losses in the life-cycle GHG emissions of a fuel-cell electric vehicle. Our review of the existing LCA studies showed that performance losses have rarely been included in the assessments. The most plausible reason for this deficiency is the scarcity of real-world data on both the durability of the cells and fuel economy of FC vehicles. As a consequence, the vast majority of the studies available in the scientific literature assume a constant fuel consumption (ranging from 0.58 to 1.15 kgH_2/100 km) for the vehicles throughout their service life, which ranges in the studies from 120,000 to 225,000 km. Nevertheless, all studies seem to agree that fuel consumption and FC durability are fundamental parameters in the life cycle impacts of a vehicle. In fact, fuel consumption is typically the main source of environmental impacts, and the performance losses of the FC are potentially a sufficient reason to replace the vehicle.

Therefore, we investigated how extending the durability of the fuel cell by replacing PTFE with FEP in the GDM would affect the greenhouse gas performance of the vehicle. Firstly, experimental results on the GDM durability were converted into parameters for the life-cycle assessment of FC vehicles. Then, the life-cycle GHG impacts of the different

vehicles were assessed based on inventories and parameters found in the scientific literature and LCA databases. Performance losses resulted in increasing the life-cycle GHG emissions of the fuel-cell electric vehicle by up to 13%. The GHG emission savings of using an FC with lower performance losses (i.e., with FEP) were negligible compared to the overall life-cycle impact of the vehicle when the service life of the vehicle was fixed at 150,000 km. Both the GDM component and amount of hydrogen saved accounted for less than 2% of the GHG emissions that arise during the vehicle operation alone. On the other hand, when the service life of the vehicle depends on the operability of the fuel cell, the global warming potential impact per driven km of the FEP-based FCEV reduces by 7 to 32%. Given the significant role that these parameters can play on the overall emissions, we advocate for the inclusion of fuel-cell durability and performance losses in future LCAs of fuel-cell electric vehicles. The range of the results depends on several variables, such as the greenhouse gas emissions from hydrogen production and the initial fuel consumption of the vehicle. Higher GHG emission savings are expected from an FC vehicle with high consumption of hydrogen produced with fossil fuels.

Our study is a first attempt to investigate the environmental implications of using an alternative coating for the GDM of fuel cells to increase their durability, with the results indicating a potential carbon footprint reduction of the fuel-cell electric vehicle. Though extensive sensitivity analysis was performed on the results, further research is necessary to improve the validity of the assessment. In particular, the durability parameters used for the LCA were based on single-cell experiments carried out in a laboratory; primary data on the durability performance and the fuel economy of the alternative fuel cell in a real vehicle are, therefore, needed. Moreover, LCA results show a real environmental benefit of using FEP only when the service life of the innovative vehicle is assumed to be longer, and the impacts are normalized per km driven. However, there is no consensus in the LCA community on the correct methodological approach to compare products with different lifetimes. Moreover, the results do not include the impacts of the maintenance of the vehicle, which could reduce the environmental benefit of extending its service life (i.e., the vehicle could require more maintenance work after 150,000 km). At the same time, the delayed emissions (e.g., the emissions from the disposal of the vehicle) were not discounted. A more thorough analysis of the potential implications of the end-of-life stage of the vehicle (e.g., recyclability of the fuel cell) is, therefore, needed.

Supplementary Materials: The following are available online at https://www.mdpi.com/article/10.3390/cleantechnol4010009/s1, Section S1: Acronyms, Section S2: Life Cycle Inventory of gas diffusion medium (GDM), Section S3: Supplementary results, Section S4: Sensitivity analysis of the effect of the fuel cell degradation rate on GWP, Table S1: Inventory of PTFE-based gas diffusion medium, Table S2: Inventory of FEP-based gas diffusion medium.

Author Contributions: Conceptualization, A.A., S.L. and G.D.; methodology, A.A. and S.L.; formal analysis, V.A., A.B.P. and S.L.; investigation, V.A., A.B.P. and S.L.; resources, G.D.; writing—original draft preparation, A.A., V.A., A.B.P. and S.L.; writing—review and editing, A.A. and A.B.P.; visualization, V.A. and A.B.P.; supervision, A.A., S.L. and G.D. All authors have read and agreed to the published version of the manuscript.

Funding: This research received no external funding.

Institutional Review Board Statement: Not applicable.

Informed Consent Statement: Not applicable.

Data Availability Statement: The data presented in this study are available on request from the corresponding author.

Acknowledgments: The authors would like to thank Sara André from the Joint Research Centre of the European Commission for her contribution to the design of the graphical abstract.

Conflicts of Interest: The authors declare no conflict of interest.

Abbreviations

AST	accelerated stress test
CNT	carbon nanotubes
DR	degradation rate
EV	electric vehicle
FC	fuel cell
FCEV	fuel cell electric vehicle
FEP	fluorinated ethylene propylene
GDL	gas diffusion layer
GDM	gas diffusion medium
GHG	greenhouse gas
GWP	global warming potential
GWP100	global warming potential over a time horizon of 100 years
HFC-23	trifluoromethane
HFP	hexafluoropropylene
ICEV	internal combustion engine vehicle
LCA	life-cycle assessment
MEA	membrane electrode assembly
MPL	microporous layer
PEMFC	proton exchange membrane FC
PTFE	polytetrafluoroethylene
TFE	tetrafluoroethylene

References

1. European Commission COM(2021) 557 Final. *Proposal for a Directive of the European Parliament and of the Council Amending Directive (EU) 2018/2001 of the European Parliament and of the Council, Regulation (EU) 2018/1999 of the European Parliament and of the Council and Direct*; European Parliament and of the Council: Brussel, Belgium, 2021.
2. Reuters. BMW, Audi among German Automakers still Betting on Fuel Cell Cars. Available online: https://europe.autonews.com/automakers/bmw-audi-among-german-automakers-still-betting-fuel-cell-cars (accessed on 10 December 2021).
3. Seemungal, L.; Arrigoni, A.; Davies, J.; Weidner, E.; Hodson, P. *Decarbonisation of Heavy Duty Vehicle Transport: Zero Emission Heavy Goods Vehicles*; No. JRC125149; Joint Reaserch Centre: Petten, The Netherlands, 2021. [CrossRef]
4. European Commission COM(2003)302. *Communication from the Commission to the Council and the European Parliament. Integrated Product Policy—Building on Environmental Life-Cycle Thinking*; European Parliament and of the Council: Brussel, Belgium, 2004.
5. Wang, C.; Wang, S.; Peng, L.; Zhang, J.; Shao, Z.; Huang, J.; Sun, C.; Ouyang, M.; He, X. Recent Progress on the Key Materials and Components for Proton Exchange Membrane Fuel Cells in Vehicle Applications. *Energies* **2016**, *9*, 603. [CrossRef]
6. Kätzel, J.; Markötter, H.; Arlt, T.; Klages, M.; Haußmann, J.; Messerschmidt, M.; Kardjilov, N.; Scholta, J.; Banhart, J.; Manke, I. Effect of ageing of gas diffusion layers on the water distribution in flow field channels of polymer electrolyte membrane fuel cells. *J. Power Sources* **2016**, *301*, 386–391. [CrossRef]
7. Hwang, J.J.; Kuo, J.K.; Wu, W.; Chang, W.R.; Lin, C.H.; Wang, S.E. Lifecycle performance assessment of fuel cell/battery electric vehicles. *Int. J. Hydrogen Energy* **2013**, *38*, 3433–3446. [CrossRef]
8. Prussi, M.; Yugo, M.; De Prada, L.; Padella, M.; Edwards, M. *JEC Well-To-Wheels Report v5*; No. JRC121213; Joint Reaserch Centre: Petten, The Netherlands, 2020. [CrossRef]
9. Hill, N.; Amaral, S.; Morgan-Price, S.; Nokes, T.; Bates, J.; Helms, H.; Fehrenbach, H.; Biemann, K.; Abdalla, N.; Jöhrens, J.; et al. *Determining the Environmental Impacts of Conventional and Alternatively Fuelled Vehicles Through LCA*; Final Report for the European Commission, DG Climate Action; European Commision: Brussel, Belgium, 2020.
10. Ahmadi, P.; Torabi, S.H.; Afsaneh, H.; Sadegheih, Y.; Ganjehsarabi, H.; Ashjaee, M. The effects of driving patterns and PEM fuel cell degradation on the lifecycle assessment of hydrogen fuel cell vehicles. *Int. J. Hydrogen Energy* **2020**, *45*, 3595–3608. [CrossRef]
11. Ahmadi, P.; Kjeang, E. Realistic simulation of fuel economy and life cycle metrics for hydrogen fuel cell vehicles. *Int. J. Energy Res.* **2017**, *41*, 714–727. [CrossRef]
12. Kaya, K.; Hames, Y. Two new control strategies: For hydrogen fuel saving and extend the life cycle in the hydrogen fuel cell vehicles. *Int. J. Hydrogen Energy* **2019**, *44*, 18967–18980. [CrossRef]
13. Latorrata, S.; Gallo Stampino, P.; Cristiani, C.; Dotelli, G. Development of an optimal gas diffusion medium for polymer electrolyte membrane fuel cells and assessment of its degradation mechanisms. *Int. J. Hydrogen Energy* **2015**, *40*, 14596–14608. [CrossRef]
14. Zhao, J.; Li, X. A review of polymer electrolyte membrane fuel cell durability for vehicular applications: Degradation modes and experimental techniques. *Energy Convers. Manag.* **2019**, *199*, 112022. [CrossRef]
15. Zhang, T.; Wang, P.; Chen, H.; Pei, P. A review of automotive proton exchange membrane fuel cell degradation under start-stop operating condition. *Appl. Energy* **2018**, *223*, 249–262. [CrossRef]

16. Wu, J.; Yuan, X.Z.; Martin, J.J.; Wang, H.; Zhang, J.; Shen, J.; Wu, S.; Merida, W. A review of PEM fuel cell durability: Degradation mechanisms and mitigation strategies. *J. Power Sources* **2008**, *184*, 104–119. [CrossRef]
17. Chun, J.H.; Jo, D.H.; Kim, S.G.; Park, S.H.; Lee, C.H.; Kim, S.H. Improvement of the mechanical durability of micro porous layer in a proton exchange membrane fuel cell by elimination of surface cracks. *Renew. Energy* **2012**, *48*, 35–41. [CrossRef]
18. Park, S.; Lee, J.-W.; Popov, B.N. A review of gas diffusion layer in PEM fuel cells: Materials and designs. *Int. J. Hydrogen Energy* **2012**, *37*, 5850–5865. [CrossRef]
19. Latorrata, S.; Stampino, P.G.; Cristiani, C.; Dotelli, G. Performance evaluation and durability enhancement of FEP-based gas diffusion media for PEM fuel cells. *Energies* **2017**, *10*, 2063. [CrossRef]
20. Latorrata, S.; Gallo Stampino, P.; Cristiani, C.; Dotelli, G. Novel superhydrophobic microporous layers for enhanced performance and efficient water management in PEM fuel cells. *Int. J. Hydrogen Energy* **2014**, *39*, 5350–5357. [CrossRef]
21. Latorrata, S.; Balzarotti, R.; Gallo Stampino, P.; Cristiani, C.; Dotelli, G.; Guilizzoni, M. Design of properties and performances of innovative gas diffusion media for polymer electrolyte membrane fuel cells. *Proc. Prog. Org. Coat.* **2015**, *78*, 517–525. [CrossRef]
22. Chen, H.; Pei, P.; Song, M. Lifetime prediction and the economic lifetime of proton exchange membrane fuel cells. *Appl. Energy* **2015**, *142*, 154–163. [CrossRef]
23. Evangelisti, S.; Tagliaferri, C.; Brett, D.J.L.; Lettieri, P. Life cycle assessment of a polymer electrolyte membrane fuel cell system for passenger vehicles. *J. Clean. Prod.* **2017**, *142*, 4339–4355. [CrossRef]
24. Benitez, A.; Wulf, C.; de Palmenaer, A.; Lengersdorf, M.; Röding, T.; Grube, T.; Robinius, M.; Stolten, D.; Kuckshinrichs, W. Ecological assessment of fuel cell electric vehicles with special focus on type IV carbon fiber hydrogen tank. *J. Clean. Prod.* **2021**, *278*, 123277. [CrossRef]
25. Huss, A.; Weingerl, P.; Mass, H.; Herudek, C.; Wind, J.; Hollweck, B.; De Prada, L.; Deix, S.; Lahaussois, D.; Faucon, R.; et al. *JEC Tank-To-Wheels Report v5: Passenger Cars*; Publications Office of the European Union: Luxembourg, 2020. [CrossRef]
26. Frank, E.D.; Elgowainy, A.; Reddi, K.; Bafana, A. Life-cycle analysis of greenhouse gas emissions from hydrogen delivery: A cost-guided analysis. *Int. J. Hydrogen Energy* **2021**, *46*, 22670–22683. [CrossRef]
27. Notter, D.A.; Kouravelou, K.; Karachalios, T.; Daletou, M.K.; Haberland, N.T. Life cycle assessment of PEM FC applications: Electric mobility and μ-CHP. *Energy Environ. Sci.* **2015**, *8*, 1969–1985. [CrossRef]
28. ISO ISO 14040. *2006 Environmental Management—Life Cycle Assessment—Principles and Framework*; International Organization for Standardization (ISO): Geneva, Switzerland, 2006.
29. ISO ISO 14044. *2006 Environmental Management—Life Cycle Assessment—Requirements and Guidelines*; International Organization for Standardization (ISO): Geneva, Switzerland, 2006.
30. IPCC. *IPCC Fifth Assessment Report (AR5)—The Physical Science Basis*; Cambridge University Press: Cambrigde, UK, 2013. [CrossRef]
31. Miotti, M.; Hofer, J.; Bauer, C. Integrated environmental and economic assessment of current and future fuel cell vehicles. *Int. J. Life Cycle Assess.* **2017**, *22*, 94–110. [CrossRef]
32. Simons, A.; Bauer, C. A life-cycle perspective on automotive fuel cells. *Appl. Energy* **2015**, *157*, 884–896. [CrossRef]
33. Rodriguez, M.A.; Van Dril, T.; Gamboa Palacios, S. *Decarbonisation Options for the Dordrecht Chemical Cluster*; The National Institute for Strategic Policy Analysis in the Fields of the Environment, Nature and Spatial Planning: Hague, The Netherlands, 2021.
34. Moon, D.J.; Kim, H.G.; Ahn, B.S.; Chung, M.J. Preparation of Hexafluoropropylene from the Pyrolysis of Trifluoromethane and Tetrafluoroethylene. U.S. Patent 6403848B1, 30 March 2001.
35. Bekel, K.; Pauliuk, S. Prospective cost and environmental impact assessment of battery and fuel cell electric vehicles in Germany. *Int. J. Life Cycle Assess.* **2019**, *24*, 2220–2237. [CrossRef]
36. Bieker, G. *A Global Comparison of the Life-Cycle Greenhouse Gas Emissions of Combustion Engine and Electric Passenger Cars*; The International Council on Clean Transportation: Washington, DC, USA, 2021.
37. International Energy Agency. *World Energy Outlook 2020*; International Energy Agency: Paris, France, 2020.
38. Argonne National Laboratory. *The Greenhouse Gases, Regulated Emissions, and Energy Use in Technologies (GREET®) Model*; Argonne National Laboratory: Argonne, IL, USA, 2021.
39. Speers, P. *Well to Wheels Report For H2ME Vehicles*; Publications Office of the European Union: Luxembourg, 2020.
40. Candelaresi, D.; Valente, A.; Iribarren, D.; Dufour, J.; Spazzafumo, G. Comparative life cycle assessment of hydrogen-fuelled passenger cars. *Int. J. Hydrogen Energy* **2021**, *46*, 35961–35973. [CrossRef]
41. Valente, A.; Iribarren, D.; Candelaresi, D.; Spazzafumo, G.; Dufour, J. Using harmonised life-cycle indicators to explore the role of hydrogen in the environmental performance of fuel cell electric vehicles. *Int. J. Hydrogen Energy* **2020**, *45*, 25758–25765. [CrossRef]
42. US Department of Energy. *FY 2017 Budget at-a-Glance*; US Department of Energy: Washington, DC, USA, 2016.
43. Kannangara, M.; Bensebaa, F.; Vasudev, M. An adaptable life cycle greenhouse gas emissions assessment framework for electric, hybrid, fuel cell and conventional vehicles: Effect of electricity mix, mileage, battery capacity and battery chemistry in the context of Canada. *J. Clean. Prod.* **2021**, *317*, 128394. [CrossRef]
44. Yang, Z.; Wang, B.; Jiao, K. Life cycle assessment of fuel cell, electric and internal combustion engine vehicles under different fuel scenarios and driving mileages in China. *Energy* **2020**, *198*, 117365. [CrossRef]
45. Usai, L.; Hung, C.R.; Vásquez, F.; Windsheimer, M.; Burheim, O.S.; Strømman, A.H. Life cycle assessment of fuel cell systems for light duty vehicles, current state-of-the-art and future impacts. *J. Clean. Prod.* **2021**, *280*, 125086. [CrossRef]
46. Hill, N.; McGraw Hill, New York, NY, USA. Personal Communication, 2021.

47. Burkhardt, J.; Patyk, A.; Tanguy, P.; Retzke, C. Hydrogen mobility from wind energy—A life cycle assessment focusing on the fuel supply. *Appl. Energy* **2016**, *181*, 54–64. [CrossRef]
48. Lombardi, L.; Tribioli, L.; Cozzolino, R.; Bella, G. Comparative environmental assessment of conventional, electric, hybrid, and fuel cell powertrains based on LCA. *Int. J. Life Cycle Assess.* **2017**, *22*, 1989–2006. [CrossRef]
49. Ren, L.; Zhou, S.; Ou, X. Life-cycle energy consumption and greenhouse-gas emissions of hydrogen supply chains for fuel-cell vehicles in China. *Energy* **2020**, *209*, 118482. [CrossRef]
50. Sinha, P.; Brophy, B. Life cycle assessment of renewable hydrogen for fuel cell passenger vehicles in California. *Sustain. Energy Technol. Assess.* **2021**, *45*, 101188. [CrossRef]
51. Velandia Vargas, J.E.; Seabra, J.E.A. Fuel-cell technologies for private vehicles in Brazil: Environmental mirage or prospective romance? A comparative life cycle assessment of PEMFC and SOFC light-duty vehicles. *Sci. Total Environ.* **2021**, *798*, 149265. [CrossRef] [PubMed]